

Effect of Annealing on Poly(urethane-siloxane) Copolymers

Jen-Taut Yeh,¹ Yao-Chi Shu²

¹Department of Polymer Engineering, National Taiwan University of Science and Technology, Taipei, Taiwan, Republic of China

²Department of Textile Engineering, Nanya Institute of Technology, Jungli, Taiwan, Republic of China

Received 23 February 2006; accepted 5 April 2006

DOI 10.1002/app.24718

Published online in Wiley InterScience (www.interscience.wiley.com).

ABSTRACT: Poly(urethane-siloxane) copolymers were prepared by copolymerization of OH-terminated polydimethylsiloxane (PDMS), which was utilized as the soft segment, as well as 4,4'-diphenylmethane diisocyanate (MDI) and 1,4-butanediol (1,4-BD), which were both hard segments. These copolymers exhibited almost complete phase separation between soft and hard segments, giving rise to a very simple material structure in this investigation. The thermal behavior of the amorphous hard segment of the copolymer with 62.3% hard-segment content was examined by differential scanning calorimetry (DSC). Both the T_1 temperature and the magnitude of the T_1 endotherm increased linearly with the logarithmic annealing time at an annealing temperature of 100°C. The typical enthalpy of relaxation was attributed to the phys-

ical aging of the amorphous hard segment. The T_1 endotherm shifted to high temperature until it merged with the T_2 endotherm as the annealing temperature increased. Following annealing at 170°C for various periods, the DSC curves presented two endothermic regions. The first endotherm assigned as T_2 was the result of the enthalpy relaxation of the hard segment. The second endothermic peak (T_3) was caused by the hard-segment crystal. The exothermic curves at an annealing temperature of above 150°C exhibited an exotherm caused by the T_3 microcrystalline growth. © 2006 Wiley Periodicals, Inc. *J Appl Polym Sci* 102: 5174–5183, 2006

Key words: poly(urethane-siloxane) copolymers; annealing; endotherm; enthalpy relaxation; exotherm

INTRODUCTION

A recent work prepared nonpolar polyurethane (PU) using polydimethylsiloxane (PDMS) as the soft segment. The nonpolar PU has better physical properties than those of polar PU (with polyether diol or polyester diol as the soft segment), including resistance to hydrolysis, thermal stability, low moisture permeability, solvent resistance, and acid/base resistance. Therefore, nonpolar PU has been employed in several applications, e.g., thermal plastic elastomers, biomaterials and fibers.^{1–4}

Linear segmented PU consists of hard and soft segments; the soft segment is typically a polyether diol or a polyester diol with a molecular weight of 500–5000. The hard segments are formed by reacting isocyanate with a diol of low molecular weight. The hard and soft segments of nonpolar PU or polar PU are immiscible; therefore, they form a two-phase structure (hard and soft phases).^{4–6} The hard phase is in a glassy or a crystalline state at room temperature; and the soft phase is in a rubber state.^{1–3} Differential scanning calorimetry (DSC) thermograms indicate that the PU has at least four phase-transition temperatures; they show two melting points (if both phases crystallize), T_{ms} and

T_{mh} , and two glass-transition temperatures, T_{gs} and T_{gh} , since PU has a two-phase structure.

The glass-transition temperature of the soft segment (T_{gs}) in polar PU usually exceeds the glass transition temperature (T_g) of pure soft-segment polymer, because soft segments are contaminated with dissolved hard segments.^{7,8} Therefore, T_{gs} increases with the hard-segment content. T_{gs} of nonpolar PU with PDMS as the soft segment is only 4–8°C higher than T_g of pure PDMS, because the decrease in free volume and chain mobility caused by the restriction of the end groups of the soft segment on the surface of the hard segment. Thus, the T_{gs} of nonpolar PU does not significantly change as the hard-segment content increases owing to the highly phase separation.⁹

The glass-transition temperature of the hard segment (T_{gh}) is very difficult to determine from DSC thermograms because of the small heat capacity of hard segment, the broad distribution of the molecular lengths, or the order of the hard segment.^{10–14} Only a few studies described the T_{gh} of polar PU copolymers. They include those of Koberstein et al.^{15,16} who investigated polar PU and suggested that a small endotherm between 50°C and 90°C in the DSC thermogram was associated with the T_{gh} of polar PU copolymers. Cuve et al.¹⁷ found a T_{gh} of nonpolar PU of ~ 106°C, which was not affected by the content or molecular weight of the hard segment, because of a highly phase separation.

Correspondence to: J.-T. Yeh (jyeh@tx.ntust.edu.tw).

TABLE I
Molar Ratio, Number-Average Molecular Weight of the Hard Segment, and Hard and Soft Segment Contents of Poly(urethane-siloxane) Copolymers

| Code | MDI/PDMS/1,4-BD (molar ratio) | Hard segment content (wt %) ¹ | Soft segment content (wt %) ² | Hard segment \bar{M}_w nh ³ | Repeating units of MDI ⁴ |
|------|----------------------------------|---|---|---|--|
| B1 | 3.5/2.5/1 | 17.6 | 82.4 | 384 | 1.5 \approx 1–2 units |
| B2 | 2/1/1 | 24.7 | 75.3 | 590 | 2.4 \approx 2–3 units |
| B3 | 3/1/2 | 34.1 | 65.9 | 931 | 3.7 \approx 3–4 units |
| B4 | 5/1/4 | 47.2 | 52.8 | 1609 | 6.4 \approx 6–7 units |
| B5 | 6.5/1/5.5 | 54.1 | 45.9 | 2122 | 8.5 \approx 8–9 units |
| B6 | 9/1/8 | 62.3 | 37.7 | 2975 | 11.9 \approx 11–12 units |

nediol (1,4-BD, $\bar{M}_w = 90$, TCI). The copolymers consisted of soft and hard segments; the soft segments comprised PDMS and the hard segments were formed by reacting MDI and 1,4-BD. An excellent blending solvent that comprised *N,N*-dimethyl-formamide (DMF, TEDIA) and tetrahydrofuran (THF, Fisher) was adopted in the synthesis. The di-*n*-butyltin dilaurate (T-12, TCI) was used as catalyst due to the weakly reactive PDMS.

Synthesis

Poly(urethane-siloxane) copolymers were synthesized in a one-step process in the blending solvent system. A 250-mL reaction flask, equipped with a stirrer, a dropping funnel and a four-way cock, was used for the polymerization. First, monomers MDI, PDMS and 1,4-BD, and a suitable blending solvent were put into the flask at 55°C and stirred for 1.5–2 h. Second, 0.02 wt % of T-12 catalyst (0.02% of the total mass of the monomer) was placed into a flask and the viscosity was then gradually increased 20 min later. Finally, DMF was added to the polymer solution stepwise to adjust the viscosity and the solvent was stirred for 2–3 h to yield the poly(urethane-siloxane) copolymers with a solid content of 30 wt %. Scheme 1 presents the synthesis of the poly(urethane-siloxane) copolymers. Table I lists the various chemical constituents and molar ratios of the copolymers applied herein.

Measurement

Fourier transform infrared spectroscopy

Samples were dissolved in DMF and then dried in an oven at 80°C for 8 h to remove the solvent and yield the desired films. The Fourier transform infrared spectroscopy (FTIR) measurements of the samples were made using a PIKE 6141 spectrophotometer operated with a scanning range of 500–4000 cm^{-1} ; the number of scans was five.

Differential scanning calorimetry

A Perkin–Elmer Pyris 1 DSC was employed to make the DSC measurements using a liquid nitrogen cooler

in an environment of helium. The indium and water were used to calibrate the temperature and heat of fusion. The masses of the samples were \sim 5–8 mg. All samples were heated from -150°C to 250°C at a heating rate of $20^\circ\text{C}/\text{min}$.

The annealing treatments were carried out with water cooling in an environment of nitrogen at above room temperature. Cyclohexane and indium were employed to calibrate the temperature and heat of fusion. All samples were first heated to 250°C at a heating rate of $20^\circ\text{C}/\text{min}$, at which temperature they were held for 1 min to remove thermal history. Then, the samples were quenched to the annealing temperature, at which they were kept for various periods. Subsequently, the samples were quenched from the annealing temperature to room temperature, at which they were maintained until the thermal equilibrium was reached. Finally, the samples were heated from room temperature to 250°C at a heating rate of $20^\circ\text{C}/\text{min}$.

The annealing-treatment conditions of the crystal exotherms were similar to the conditions described above. After the thermal history was removed, the samples were quenched to the annealing temperature at which they were maintained for 3 h. Then, the

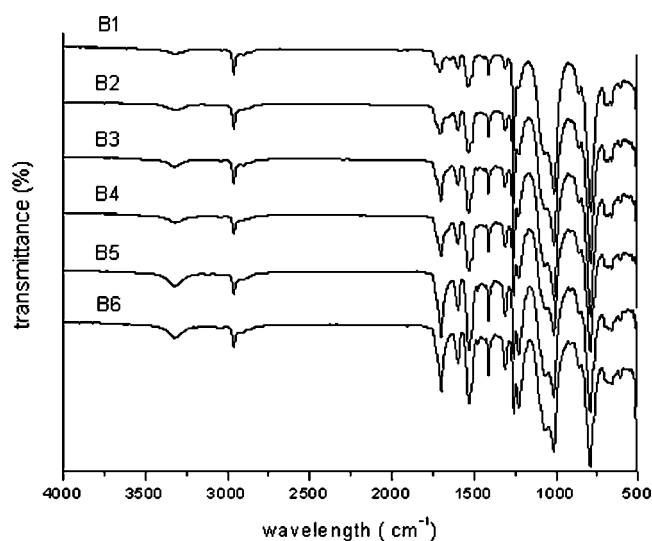


Figure 1 The FTIR spectra of copolymers.

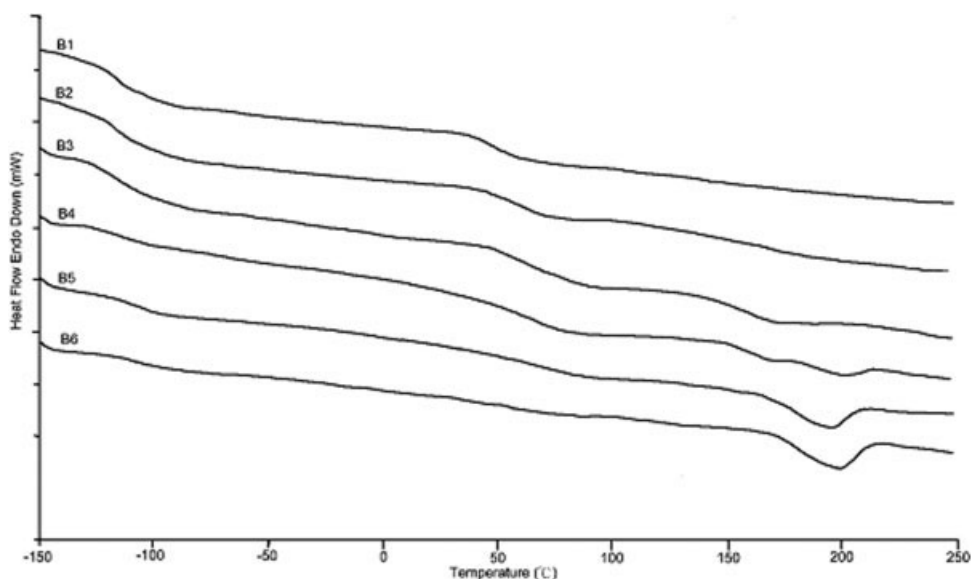


Figure 2 DSC thermograms of copolymers heated from -150°C to 250°C .

samples were heated from the annealing temperature to 250°C at a heating rate of $20^{\circ}\text{C}/\text{min}$.

Wide-angle X-ray diffraction pattern

Samples were cut into $3\text{ cm} \times 3\text{ cm}$ squares and placed on a DLANO 8536 X-ray diffractometer. The X-ray beam was nicked-filtered Cu-K α radiation from a sealed tube operated at a voltage of 30 kV and a current of 10 mA.

RESULTS AND DISCUSSION

Fourier transform infrared spectroscopy

Figure 1 presents the transmission FTIR spectra of poly(urethane-siloxane) copolymers prepared from OH-terminated PDMS, 1,4-BD and MDI. The characteristic absorption band of the urethane hard segment is displayed at 3300 cm^{-1} ($-\text{NH}$ stretching) and 1700 cm^{-1} ($\text{C}=\text{O}$ contracting). The characteristic absorption band of the PDMS soft segment is at 1260 cm^{-1} ($-\text{CH}_3$ bending), 1020 cm^{-1} and 1100 cm^{-1} ($-\text{Si}-\text{O}-\text{Si}-$ bending), and 860 cm^{-1} and 810 cm^{-1} ($-\text{CH}_3$ rocking). The spectra indicate that these copolymers have urethane and siloxane structures.

Phase transition regions of poly(urethane-siloxane) copolymers

Figure 2 displays the DSC thermogram of poly(urethane-siloxane) copolymers at the heating rate of $20^{\circ}\text{C}/\text{min}$. Table II presents the phase transition temperatures of the samples. Two to four transition regions are observed in the DSC curves. The soft-phase

transition region of PDMS appears between -116°C and -119°C , and the phase is amorphous. The temperature of the phase transition is regarded as the glass-transition temperature of PDMS soft segment (T_{gs}). The hard phase comprises the urethane segment formed from the reaction of MDI and 1,4-BD. The hard-phase transitions occur beyond room temperature and have several endothermic regions at T_1 , T_2 , and T_3 .

Soft phase

The glass-transition temperature (T_g) of pure PDMS is -123°C ,⁴ but the T_{gs} of copolymers used PDMS as soft segment exceeds the T_g because a little mixing occurs between soft and hard segments. Therefore, the T_g value can be used as an indication of the relative purity of the soft segment.^{7,25} Greater contamination of the soft domains (soft phase) with dissolved hard segments corresponds to higher T_{gs} . The T_{gs} of all samples are kept almost constant at about -117°C as the hard-segment content increases from 17.6% to 62.3%, as shown in Tables I and II. This result reveals the high

TABLE II
Phase Transition Regions of Poly(urethane-siloxane) Copolymers

| Code | T_{gs} ($^{\circ}\text{C}$) | T_1 ($^{\circ}\text{C}$) | T_2 ($^{\circ}\text{C}$) | T_3 ($^{\circ}\text{C}$) | ΔH (J/g) |
|------|--|------------------------------|------------------------------|------------------------------|------------------|
| B1 | -116 | 50 | - | - | - |
| B2 | -117 | 63 | 158 | - | - |
| B3 | -117 | 62 | 170 | - | - |
| B4 | -116 | 65 | 174 | 212 | 4.415 |
| B5 | -119 | 82 | - | 191 | 38.508 |
| B6 | -117 | 76 | - | 202 | 39.574 |

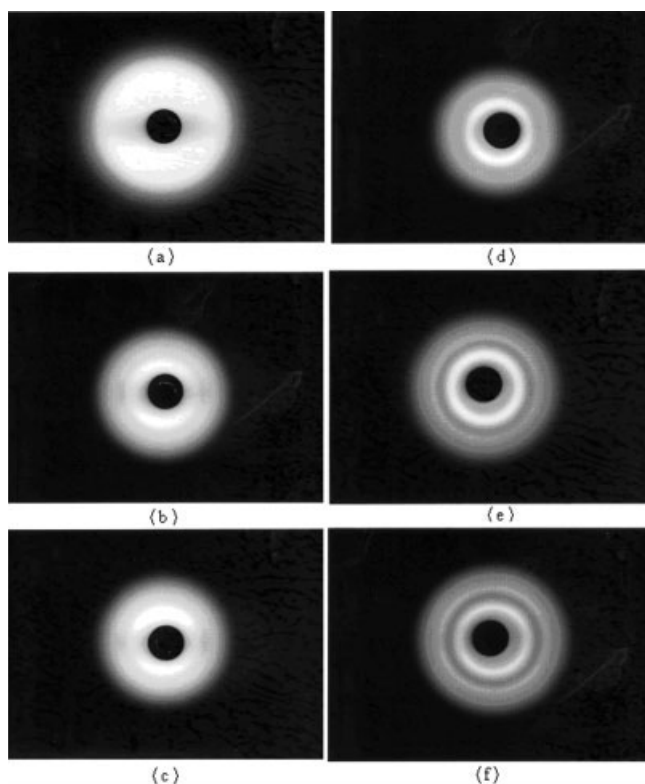


Figure 3 Wide-angle X-ray diffraction patterns of copolymers (a) B1, (b) B2, (c) B3, (d) B4, (e) B5, and (f) B6.

phase separation of the copolymers. Thus, the hard segments are separated from the soft domains, causing the hard segments to form another hard domain.

Although the melting temperature of the soft segment (T_{ms}) of typical PU is around 20°C , the T_{ms} of poly(urethane-siloxane) copolymers are absent because the PDMS soft segment cannot crystallize. The result is

attributable to the stereo hindrance resulting from the benzene ring of MDI and the fact that the $-\text{Si}-\text{O}-$ main chain is hindered by the methyl side group.

Hard phase

Three endothermic regions in the DSC thermogram related to the hard phase and depended upon many factors, such as the hard-segment content, as well as the conformation and length of the hard segment.¹⁸ The B1 sample in this study exhibits only a clear T_1 endotherm at around 50°C , indicating that the B1 sample has only a short-range ordered hard segment because the average molecular weight of the hard segment of sample B1 is 384. Since the average molecular weight equals one to two repeating units of MDI, the sample cannot form the long-range ordered hard segment (T_2) and the crystal region (T_3). Therefore, T_2 and T_3 endothermic regions of the B1 sample are absent from the DSC thermogram, as shown in Figure 2. The T_1 endotherm of the B2 sample appears at around 63°C , which exceeds that of the B1 sample, suggesting that the B2 sample has a finer short-range ordered structure. Similarly, the T_2 endotherm of the B2 sample is also unclear, because the hard segment is shorter, as shown in Figure 2. Therefore, when a sample has just more than two repeating units of MDI, those long hard-segment units (long units of MDI) can be gathered to form the long-range ordered structure (Region II). Since B3 and B4 samples contain more hard segments than B1 and B2 samples, their T_1 and T_2 endothermic regions appear at about 65°C and 170°C , respectively. In fact, both samples have sufficiently long MDI units, and so show better Regions I and II. Furthermore, the B4 sample presents a board endothermic peak (T_3) at around 210°C and a melting

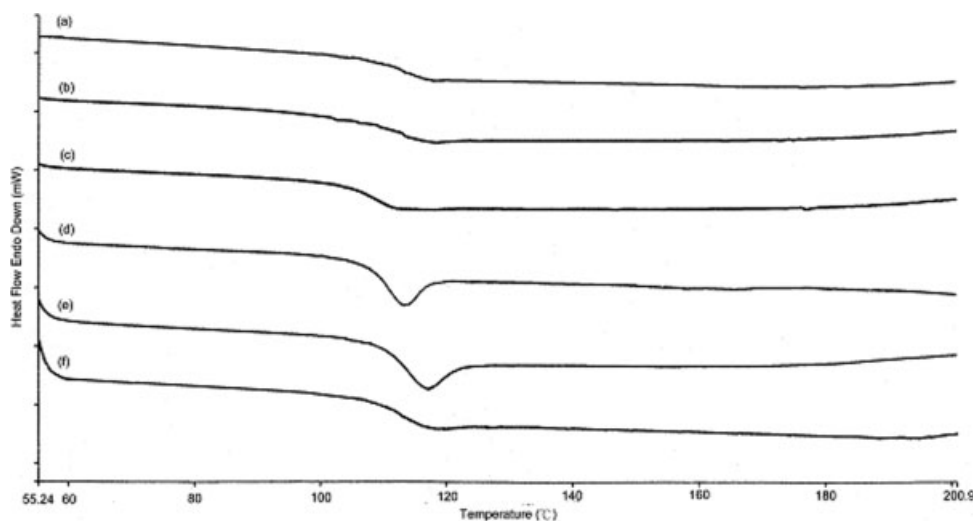


Figure 4 DSC thermogram of B6 sample heated from room temperature to 200°C after annealing at various temperatures (T_a) for 3 h (a) $T_a = 60^{\circ}\text{C}$, (b) $T_a = 70^{\circ}\text{C}$, (c) $T_a = 80^{\circ}\text{C}$, (d) $T_a = 90^{\circ}\text{C}$, (e) $T_a = 100^{\circ}\text{C}$, and (f) $T_a = 110^{\circ}\text{C}$.

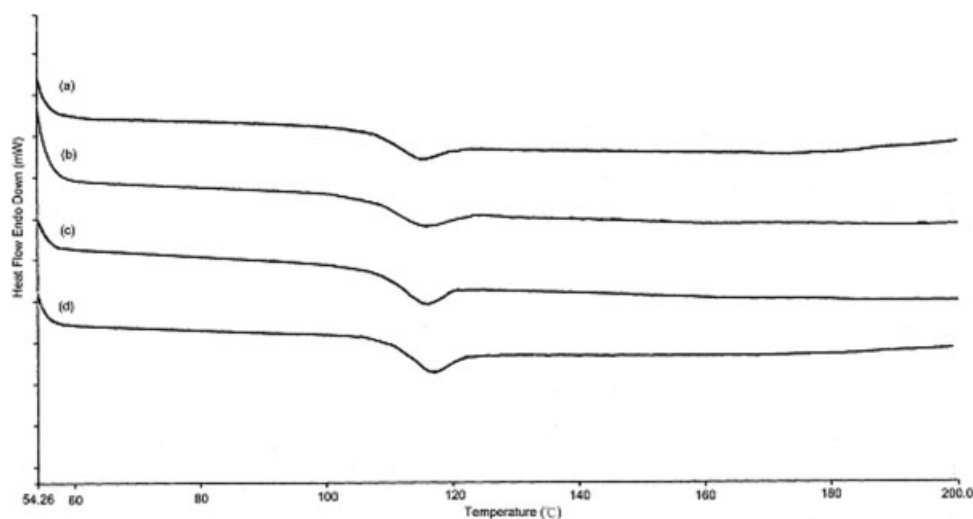


Figure 5 DSC thermogram of B6 sample heated from room temperature to 200°C after annealing at 100°C for various periods (a) $t_a = 30$ min, (b) $t_a = 1$ h, (c) $t_a = 2$ h, and (d) $t_a = 3$ h.

enthalpy (ΔH) of the peak of 4.415 J/g. Clear T_3 endotherms are observed at 191°C and 202°C with ΔH of 38.508 and 39.574 J/g for the B5 and B6 samples, respectively. The results show that the crystallization of the poly(urethane-siloxane) copolymers occurs when the sample has a hard-segment content of over 47.2 wt %. T_2 and T_3 endotherms of both samples (B5 and B6) overlap and cannot be measured because the T_3 endotherms are large and broad. Petrovic²⁶ studied the crystalline of polar PU and indicated that the DSC thermogram shows clear melting endotherms when the average molecular weight of the hard segment exceeded 8000 (equal to about thirteen MDI repeating units). However, the average molecular weight of the hard segment for the B5 sample is only 2122 (about eight to nine repeating MDI units) in this study, and the DSC thermogram exhibited a clear melting endothermic peak, revealing that a strong phase separation occurs between the soft and hard segments; therefore, the hard segments aggregate to form the ordered structure. Thus, the poly(urethane-siloxane) copolymers with a lower hard-segment content can have the crystalline of hard phase. Hence, the DSC curves of poly(urethane-siloxane) copolymers with a low hard-segment content have one to two endotherms (T_1 and T_2). A third endotherm appears for samples with hard segments that are sufficiently long to form hard-segment crystallization.

Figure 3 presents the wide-angle X-ray diffraction pattern of copolymers. The diffraction patterns of B1, B2, and B3 samples are almost amorphous, and may be included in Regions I and II. The results are consistent with previous DSC analyses. Furthermore, the diffraction patterns of B4, B5, and B6 samples exhibit semicrystalline structures and indicate that the crystallinity and degree of orientation increase with the hard-segment content. This result shows that a poly(urethane-siloxane)

copolymer with a higher hard-segment contents has a better ordered structure of Region III.

Effect of annealing on the hard phase content

Figure 2 and Table II indicate that the B6 sample with high hard-segment content shows clear Region I, II and III structures. The B6 sample is employed to examine the effect of annealing on the hard phase of the poly(urethane-siloxane) copolymer and thereby study the thermal behavior of its hard segment.

Effect of low-temperature annealing

Figure 4 displays the DSC thermograms of the B6 sample heated from room temperature to 200°C at a rate of 20°C/min after annealing at various temperatures (T_a) for 3 h. The DSC curves for $T_a = 60^\circ\text{C}$, 70°C , 80°C , and 110°C represent endothermic regions at about 110–120°C, as shown in Figure 4. However, the endothermic peak appears at 115.4°C with $\Delta H = 2.112$ J/g for $T_a = 90^\circ\text{C}$, and at 118.8°C with $\Delta H = 2.275$ J/g for $T_a = 100^\circ\text{C}$. The endothermic peak is largest at $T_a \approx T_{\text{gh}} - 20^\circ\text{C}$, i.e., $100^\circ\text{C} \approx 118.8^\circ\text{C} - 20^\circ\text{C}$.

Figure 5 depicts sample B6 annealed at 100°C for various periods (t_a). The magnitude and temperature of the endothermic peak increase with t_a . Table III

TABLE III
Endothermic Temperatures and ΔH of B6 Sample after Annealing at 100°C for Various Periods

| Code | ΔH (J/g) | Temperature (°C) |
|--------|------------------|------------------|
| 30 min | 1.510 | 115.0 |
| 1 h | 1.586 | 115.1 |
| 2 h | 1.983 | 115.8 |
| 3 h | 2.266 | 116.8 |

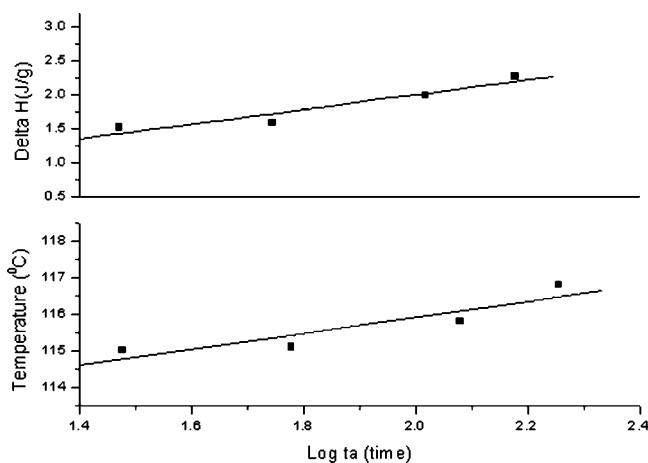


Figure 6 Relationships between both temperature and magnitude (ΔH) of endothermic peak, and the logarithm of t_a ($\log t_a$).

shows the peak values are from 115°C to 116.8°C and the ΔH increases from 1.510 to 2.266 J/g, suggesting that numerous and great ordered structures (Region I) are formed during annealing. In fact, Region I structures of the copolymers are improved by annealing. According to previous reports,^{20,21,27,28} the T_1 endotherm appeared at around 50–140°C under different annealing times (t_a) or annealing temperatures. In this study, T_1 endotherms of poly(urethane-siloxane) copolymers are present at about 115°C at an annealing temperature of 100°C for various periods. Furthermore, the endothermic temperature and ΔH are linearly related to the logarithm of t_a ($\log t_a$), as shown in Figure 6.

Physical aging is a thermodynamic nonequilibrium process of the glassy state. Molecules cannot reach their equilibrium conformation, because of the rapid

increase in viscosity and the decrease in molecular mobility during cooling through T_g . The thermodynamic potential for the molecules approach equilibrium state. The enthalpy and volume of the amorphous polymer have been determined to decrease as t_a increases. Tenbrinke and Grooten²⁹ attributed enthalpy relaxation behaviors to the aging of the amorphous polymers and drew the following conclusions.

1. The magnitude of the endotherm peak in the proximity of T_g increases linearly with $\log t_a$, when the aged glass is not in equilibrium.^{30–32}
2. Under the same conditions, the position of the endotherm peak also increases linearly with $\log t_a$.^{30,33,34}
3. The maximum magnitude of the endotherm peak is a function of T_a when $T_a = T_{gh} - 20^\circ\text{C}$.^{33,35}

Comparing our results with those statements demonstrates that the T_1 endothermic behavior of the B6 sample under low-temperature annealing is the enthalpy relaxation behavior associated with the physical aging of the amorphous urethane hard segment.

Effect of high-temperature annealing

According to the preceding section, the endothermic peak of poly(urethane-siloxane) copolymers at an annealing temperature below 110°C is associated with enthalpy relaxation behavior of amorphous hard segments. Complete Region I structures can be formed by annealing below 110°C. However, Figures 4 and 5 show that the Region II structures are not further improved by annealing at 100°C, because the long-range ordered hard segment is not disrupted under the lower-temperature annealing conditions. There-

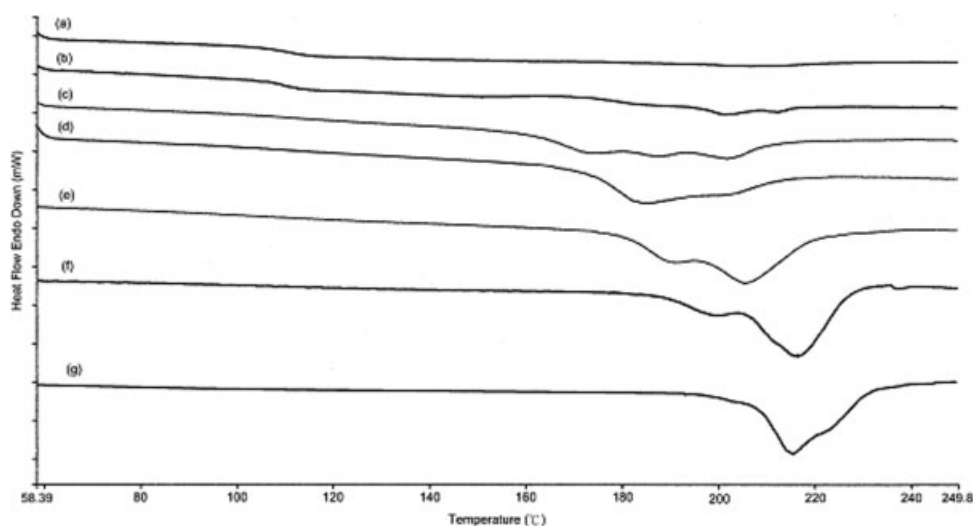


Figure 7 DSC thermogram of the B6 sample heated from room temperature to 250°C after annealing at various temperatures (T_a) for 3 h (a) $T_a = 120^\circ\text{C}$, (b) $T_a = 130^\circ\text{C}$, (c) $T_a = 140^\circ\text{C}$, (d) $T_a = 150^\circ\text{C}$, (e) $T_a = 160^\circ\text{C}$, (f) $T_a = 170^\circ\text{C}$, and (g) $T_a = 180^\circ\text{C}$.

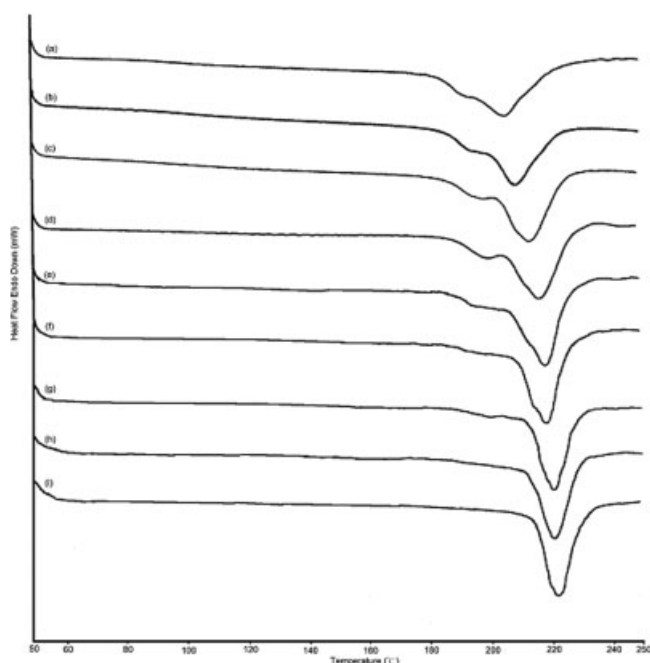


Figure 8 DSC thermogram of B6 sample heated from room temperature to 250°C after annealing at 170°C for various periods (a) $t_a = 30$ min, (b) $t_a = 1$ h, (c) $t_a = 2$ h, (d) $t_a = 3$ h, (e) $t_a = 12$ h, (f) $t_a = 24$ h, (g) $t_a = 48$ h, (h) $t_a = 72$ h, and (i) $t_a = 120$ h.

fore, the Region II structure cannot reform and re-order under this annealing condition. The B6 sample was further annealed at higher temperatures to investigate the Region II structure and the T2 endothermic behavior.

Figure 7 displays the DSC thermograms of the B6 sample after annealing between 120°C and 180°C for 3 h. Some endothermic peaks appear between 160°C and 200°C and are termed T_2 endotherms (Region II), as shown in Figure 7(c–f); they are caused by the

long-range ordered hard segment. The endothermic peaks, associated with the hard-segmented crystal (Region III), appear at above 200°C.¹⁸ Moreover, a small endothermic region (T_1) is evident at about 100–120°C following annealing at a temperature of 120–130°C for 3 h, as shown in Figure 7(a and b). The T_1 endothermic region gradually disappears as the annealing temperature is increased, as shown in Figures 7(c and g). The T_1 endothermic region gradually approaches the T_2 endothermic region until the T_1 endothermic region merges with the T_2 endothermic region. Finally, those endothermic peaks form a large endothermic peak around 215°C following annealing at 180°C for 3 h, as shown in Figure 7(g). The results demonstrate that the short-region ordering of hard segments (Region I structure) can form long-region ordering of hard-segments (Region II structure) following higher-annealing temperature and the crystal structure (Region III structure).

The endothermic peaks appeared at 180–200°C following annealing at 150–170°C (consistent with the relationship, $T_a = T_{gh} - 20^\circ\text{C}$), as shown in Figure 7(d–f). We suggest that the result may be caused by the enthalpy relaxation during annealing. The multiple endothermic peaks [Fig. 7(b–f)] disappear and merges to a broad peak at $T_a = 180^\circ\text{C}$, revealing that Region I merges with Region II, and then Region II aggregates to form Region III, at an annealing temperature of above 180°C, as shown in Figure 7(g). The ΔH values of the T_2 endotherms at $T_a = 150^\circ\text{C}$, 160°C, and 170°C are nearly the same, as shown in Figure 7, but the temperature of T_2 endotherm increases with T_a to an annealing temperature of 180°C, at which the T_2 endotherm disappears and merges into T_3 . Clearly, higher-temperature annealing does not promote the development of a Region II structure, but, rather, the growth of the Region II structure to a Region III structure. Clearly,

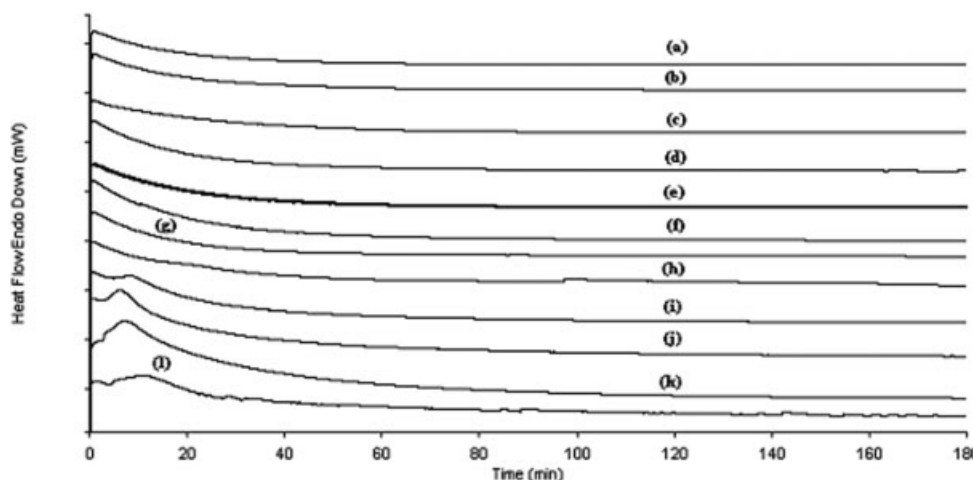


Figure 9 Isothermally exothermic curves of B6 sample annealed at various temperatures (T_a) for 3 h. (a) $T_a = 80^\circ\text{C}$, (b) $T_a = 90^\circ\text{C}$, (c) $T_a = 100^\circ\text{C}$, (d) $T_a = 110^\circ\text{C}$, (e) $T_a = 120^\circ\text{C}$, (f) $T_a = 130^\circ\text{C}$, (g) $T_a = 140^\circ\text{C}$, (h) $T_a = 150^\circ\text{C}$, (i) $T_a = 160^\circ\text{C}$, (j) $T_a = 170^\circ\text{C}$, (k) $T_a = 180^\circ\text{C}$, and (l) $T_a = 190^\circ\text{C}$.

the maximum temperature of the T_2 endotherm appears at $T_a = 170^\circ\text{C}$.

Effect of isothermal annealing

The B6 sample was further annealed at 170°C for various annealing periods (t_a) to examine the effect of annealing time at higher temperature on the hard-segment morphology. Figure 8 displays two endothermic regions. The first endotherm, which is regarded as Region II, appears at about 190°C (just 20°C above the annealing temperature), probably, as mentioned above, because of the enthalpy relaxation of the hard segment caused by physical ageing. The second endothermic peak (T_3) is 40°C higher than the annealing temperature and is associated with hard-segment crystal. However, a tiny shoulder appears in the front of the T_3 endotherm, as shown in Figure 8(c and d). According to previous studies,^{20,21} the tiny shoulder corresponds to the re-association of mobile hard

segments and disordered hard segments, which move into Region III after a long period at a high annealing temperature. Figure 8 displays the magnitude of T_3 endotherm increases with t_a and the position of the T_2 peak, and a tiny shoulder disappears, as t_a increases over 120 h. The results indicate that the long-region ordering hard segments (Region II) could move into the crystalline regions (Region III) under prolonged higher-temperature annealing. Purer crystalline poly(urethane-siloxane) copolymers with 62.3 wt % hard-segment content have a t_a and T_a of at least 170°C and 120 h, respectively.

Crystallization temperature and phase transition region

The B6 sample was annealed at various temperatures for 3 h, as shown in Figure 9 to determine the crystallization temperature of the poly(urethane-siloxane) copolymers. The crystallization temperature of the

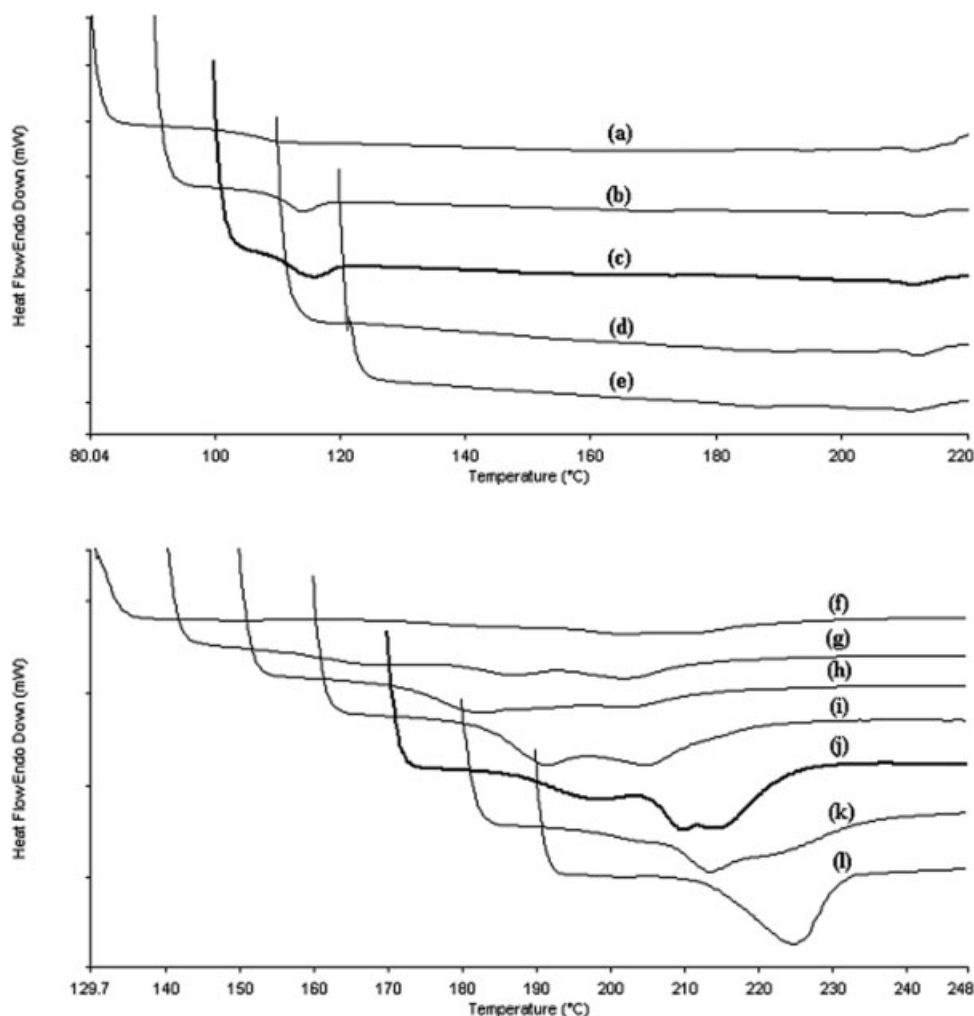


Figure 10 DSC thermograms of B6 sample heated from annealing temperatures to 250°C after annealing at different temperatures for 3 h (a) $T_a = 80^\circ\text{C}$, (b) $T_a = 90^\circ\text{C}$, (c) $T_a = 100^\circ\text{C}$, (d) $T_a = 110^\circ\text{C}$, (e) $T_a = 120^\circ\text{C}$, (f) $T_a = 130^\circ\text{C}$, (g) $T_a = 140^\circ\text{C}$, (h) $T_a = 150^\circ\text{C}$, (i) $T_a = 160^\circ\text{C}$, (j) $T_a = 170^\circ\text{C}$, (k) $T_a = 180^\circ\text{C}$, and (l) $T_a = 190^\circ\text{C}$.

exotherms was obtained at a T_a of over 150°C, and the maximum peak appeared at $T_a = 170^\circ\text{C}$. Figure 10 is similar to Figure 9, but is obtained with quenching to the annealing temperatures followed by heating from the T_a to 250°C. The melting peak (T_3) was observed above 150°C and the crystallization enthalpy was maximal at about 190°C. Notably, the DSC curves also revealed the temperatures of phase transitions among Regions I, II and III, during which Region I (T_1) merges with Region II (T_2), and Region II (T_2) merges with Region III. The T_1 peak appeared at a T_a of between 80°C and 100°C, which increased with the annealing temperature. However, the T_1 peak almost disappeared at a T_a of between 110°C and 120°C, as shown Figure 10. As the T_a increases above 130°C, the T_2 peak obviously appears at 180°C and the T_3 peak is also presented at above 200°C. As T_a increases, the T_2 peak gradually becomes associated with the T_3 peak until $T_a = 190^\circ\text{C}$, at which temperature the process ends. The results indicate that Region I form when T_a is below 110°C, but it is gradually merged into Region II when T_a exceeds 110°C. Subsequently, the Region II becomes associated with Region III at a T_a of over 140°C and the maximum melting endotherm appears at 190°C. Notably, the annealing temperature (T_a) is maintained for 3 h.

CONCLUSIONS

Segmented poly(urethane-siloxane) copolymers were synthesized using MDI and 1,4-BD as hard segments and PDMS as the soft segment. DSC analysis showed that the copolymers exhibited strong phase separation, since the T_{gs} of copolymers were uniform under various hard-segment molecular weights and various hard-segment contents. The copolymers clearly exhibited T_1 , T_2 , and T_3 endotherms when the hard-segment content exceeded 47.2 wt %. The B6 sample was used to investigate T_1 , T_2 , and T_3 endotherms by annealing treatment. Low-temperature annealing treatment demonstrated that the magnitude and the temperature of the T_1 endotherm were linearly related to the logarithm of the annealing time, suggesting that the T_1 endotherm corresponded to enthalpy relaxation behavior resulting from the physical aging process. Following high-temperature annealing treatment, the T_2 endotherm appeared at between 160°C and 200°C, and was enthalpy relaxation. T_1 and T_2 were mobile under higher-temperature annealing. As the annealed temperature increased, T_1 merged with T_2 ; however, the magnitude of the T_2 endotherm was almost constant as the annealing temperature declined below 170°C. Regions I and II (T_1 and T_2) following higher-temperature annealing at over 170°C for 120 h, were associated with Region III (T_3). The curves obtained by

maintaining various temperatures for 3 h exhibited an exothermic peak at annealing temperatures of above 150°C, indicating that the Region II structure grew into the Region III structure.

References

- Gibson, P. E.; Vallance, M. A.; Cooper, S. L. Development in Block Copolymer, Applied Science Series; Elsevier: London, 1982.
- Hepburn, C. Polyurethane Elastomers, Applied Science Series; Elsevier: London, 1982.
- Aggarwal, S. L. Block Polymer; Plenum: New York, 1970.
- Speckhard, T. A.; Hwang, K. K. S.; Cooper, S. L.; Chang, V. S. C.; Kennedy, J. P. Polymer 1985, 26, 70.
- Speckhard, T. A.; Ver Strate, G.; Gibson, P. E.; Cooper, S. L. Polym Eng Sci 1983, 23, 337.
- Schneider, N. S.; Matton, W. Polym Eng Sci 1979, 19, 1122.
- Petrovic, Z. S.; Soda-So, I. J. J Polym Sci Part B: Polym Phys 1989, 27, 545.
- Van-Bogart, J. W. C.; Gibson, P. E.; Cooper, S. L. J Polym Sci Polym Phys Ed 1983, 21, 65.
- Xu, Y.; Nagarajan, M. R.; Grasel, T. G.; Gibson, P. E.; Cooper, S. L. J Polym Sci Polym Phys Ed 1985, 23, 2319.
- Speckhard, T. A.; Hwang, K. K. S.; Yang, C. Z.; Laupan, W. R.; Cooper, S. L. J Macromol Sci Phys 1984, 23, 175.
- Yang, C. Z.; Hwang, K. K. S.; Cooper, S. L. Macromol Chem 1983, 184, 651.
- Camberlin, Y.; Pascault, J. P.; Letoffe, M.; Claudy, P. J Polym Sci Polym Phys Ed 1982, 20, 1445.
- Li, Y.; Gao, T.; Liu, J.; Linliu, K.; Desper, C. R.; Chu, B. Macromolecules 1992, 25, 7365.
- Koberstein, J. T.; Galambos, A. F. Macromolecules 1992, 25, 5618.
- Koberstein, J. T.; Galambos, A. F.; Leung, L. M. Macromolecules 1992, 25, 6195.
- Koberstein, J. T.; Leung, L. M. Macromolecules 1992, 25, 6205.
- Cuve, L.; Pascault, J. P.; Boiteux, G. Polymer 1992, 33, 3957.
- Seymour, P. W.; Cooper, S. L. Macromolecules 1973, 6, 48.
- Hesketh, T. R.; Van-Bogart, J. W. C.; Cooper, S. L. Polym Eng Sci 1980, 20, 190.
- Leung, L. M.; Koberstein, J. T. Macromolecules 1986, 19, 706.
- Koberstein, J. T.; Russell, T. P. Macromolecules 1986, 19, 714.
- Hu, W.; Koberstein, J. T. J Polym Sci Part B: Polym Phys 1994, 32, 437.
- Koberstein, J. T.; Stein, R. S. J Polym Sci Polym Phys Ed 1983, 21, 1439.
- Chen, T. K.; Shieh, T. S.; Chui, J. Y. Macromolecules 1998, 31, 1312.
- Speckhard, T. A.; Gibson, P. E.; Cooper, S. L.; Chang, V. S. C.; Kennedy, J. P. Polymer 1985, 26, 55.
- Petrovic, Z. S.; Budinski-Simendic. J Rubber Chem Technol 1985, 58, 685.
- Van-Bogart, J. W. C.; Bluemke, D. A.; Cooper, S. L. Polymer 1981, 22, 1428.
- Galambos, A. F.; Koberstein, J. T. Polym Mater Sci Eng 1989, 61, 359.
- Tenbrinke, G.; Grooten, R. Colloid Polym Sci 1989, 267, 992.
- Richardson, M. J.; Savill, N. G. Polymer 1977, 18, 413.
- Ellis, T. S. Macromolecules 1990, 23, 1494.
- Agrawal, A. J Polym Sci Part B: Polym Phys 1989, 27, 1449.
- Hodge, I. M.; Berens, A. R. Macromolecules 1982, 15, 762.
- McGowan, C. B.; Kim, D. Y.; Blumstein, R. B. Macromolecules 1992, 25, 4568.
- Hodge, I. M. Macromolecules 1983, 16, 898.